

IMPACT OF BOOKING LEAD TIME ON FLEET AND INFRASTRUCTURE IN URBAN AIR MOBILITY

Majed Swaid[1]

[1]German Aerospace Center (DLR), Institute of Air Transport, 21079 Hamburg, Germany.

Abstract

In this study, an existing model for mission assignment and fleet sizing in an urban air mobility network is extended by incorporating a rolling-horizon approach. The method is used to simulate mission bookings that arrive continuously throughout the day and to optimize fleet operations from an operator's perspective. The aim of the study is to quantify the influence of booking lead time on fleet size, operational efficiency, and infrastructure requirements. To this end, the booking lead time is varied between 60 and 180 minutes, and the resulting fleets and operating schedules are analyzed using various metrics. The results show that booking lead time has a significant impact on fleet size as well as on vehicle utilization over time. At a booking lead time of 120 minutes, the required fleet size can be reduced by up to 17% while maintaining identical transport demand in the investigated network in Hamburg, Germany. At the same time, this fleet reduction is accompanied by only a 3% increase in total energy demand. The results quantify the operational value of demand information by assessing the trade-offs between fleet size, energy demand, and booking lead time. Since booking lead time directly influences passenger flexibility, it also affects the perceived service quality.

Keywords: Fleet Sizing, Booking Lead Time, Infrastructure Requirements, Demand Pattern Analysis, Advanced/Innovative Air Mobility

1. Introduction

The concept of Urban Air Mobility (UAM) promises a reduction in travel times, as long as certain prerequisites are fulfilled. For instance, vertiports must be located close to the passenger to reduce access and egress distances, thereby minimizing total travel time. The linking of network density and vertiport positions with UAM demand has been the subject of prior research [1–3]. Further analyses have focused on UAM ground infrastructure design, such as the performance of specific vertiport topologies [4–5] and approach procedures [6].

Building upon the findings related to these individual aspects of the UAM system, the question arises as to how fleet and infrastructure requirements evolve when considering the network as a whole. Combining results as input and integrating into a network perspective, overarching studies have conducted analyses regarding requirements for fleet size and local ground infrastructure capacity based on specific demand scenarios. In [7], for example, an approach was demonstrated for a specific Ohio-based case study, selecting the best vertiport positions and the number of air taxi allocations while minimizing costs. A holistic UAM network optimization based on a London case study was presented in [8], introducing a three-stage algorithm which first places vertiport locations. Subsequently, the vertiports are specified using a vertiport sizing model to derive the required take-off, landing, and charging pads at each vertiport. Another approach for the integrated design of the vertiport network and fleet design requirements was presented in [9,10], in which the local ground infrastructure requirements, such as for charging, parking and maintenance, were analyzed based on a Hamburg-based commuter traffic scenario. The analysis and optimization of UAM networks is crucial to assess transport capacity and to derive suitable design strategies for both vertiports and vehicles. Since the actual requirements resulting from future use cases are not yet known, studies usually present analyses for specific scenarios with selected showcase cities and various

https://doi.org/10.71945/icas2026_0672

assumptions regarding the analyzed use cases. Existing studies have primarily focused on the optimization of fleet composition, vertiport placement, and infrastructure sizing for predefined demand scenarios. However, less attention has been paid to the influence of operational characteristics such as booking lead time and demand concentration on the resulting fleet and infrastructure requirements.

This study analyzes the sensitivity of fleet and ground infrastructure requirements with respect to the permissible booking lead time t_{BL} of a flight. Furthermore, this influence is quantified for two demand patterns that are similar with respect to overall transport demand and its temporal distribution, but differ in the spatial concentration of demand at individual vertiports.

There are many use cases for air taxis in which demand occurs spontaneously — for instance, in the field of private leisure trips or in business, when the occurrence of a trip is certain but its timing remains flexible within the day. From the passenger's perspective, a shorter t_{BL} of only a few minutes is an indicator of service quality, as it enables spontaneous bookings. From the operator's perspective, however, small values of t_{BL} may be disadvantageous, as they restrict efficient planning of vehicle rotations and may consequently increase idle times and require larger fleets. On the other hand, several use cases are moderately predictable, such as commuting or airport feeder services, which do not necessarily require short booking lead times but can involve demand peaks in the form of rush hours. The influence of t_{BL} is quantified using key performance indicators, including fleet size, vehicle idle time, energy demand and infrastructure requirements.

2. Methodology

2.1 General Assumptions

The goal of the developed method is to quantify transport efficiency in a UAM network based on the lead time of a mission booking made by the passenger. In this context, efficiency can be evaluated in terms of temporal vehicle utilization and seat utilization.

If, for example, the operator receives a flight booking well in advance (e.g., three hours) of the desired departure time, it is possible to adjust the rotations of individual vehicles in such a way as to increase transport efficiency. Depending on the chosen metric, this can be achieved, for example, by minimizing the number of empty flights or empty seat-kilometers. This applies in particular to cases where relocation flights are required or a vehicle with significantly more seats than the travel group comprises is deployed. If, on the other hand, the operator is only notified of a mission shortly before the scheduled departure (e.g., 60 minutes), there are significantly fewer options for rescheduling vehicle deployment, as suitable vehicles may not be in proximity or may not have sufficient battery charge.

The model builds on the method presented in [9], which describes an integrated process for translating demand scenarios into vehicle rotations and successively building fleet pools until all missions in the pool have been assigned on a one-to-one basis. To make the assignment problem manageable, possible operational plans for vehicle rotations are first created using a graph-based approach, each representing a candidate vehicle. Subsequently, additional candidates are selected in each iteration by solving a MILP (Mixed-Integer Linear Program). Each of these candidates represents a potential vehicle in the fleet pool. The following section describes the selected constraints for creating and selecting these sequences. Subsequently, the model adjustments made to account for the pool of transport requests that develops successively over the course of the day are explained.

The investigated network consists of 20 vertiport locations in Hamburg, Germany. The positioning of the vertiports is not part of this study; instead, the locations are taken from [9]. These are located in proximity to demand hotspots. Furthermore, all vertiports are assumed to be at a reference elevation of 0 m, so that topographical differences between the locations are neglected.

The demand scenarios analyzed in this study are based on the scenarios first introduced in [12,13].

Both scenarios are derived from commuter and business travel demand, albeit in different proportions. Based on these assumptions, traffic patterns with two pronounced rush-hour periods were generated (see Fig. 1). To ensure a meaningful comparison of fleet and infrastructure requirements, both scenarios were scaled to a similar demand level of approximately 2,400 missions per day.

Each mission in the demand pool is defined by a fixed departure time, a start and destination vertiport, and the number of passengers. Therefore, there is no flexible adjustment of travel groups, such as merging or splitting different groups.

Furthermore, delays resulting from potential operational disruptions are not explicitly accounted for. Instead, such effects are modeled using fixed time buffers for boarding, deboarding, and taxiing. Based on the metrics displayed in Fig. 1, the scenarios appear to be very similar. However, they differ with respect to the composition of travel demand. While Scenario A is dominated by commuter traffic, Scenario B assumes a higher share of business-related travel. Although both scenarios exhibit similar overall demand characteristics, the temporal distribution of missions at individual vertiports differs, resulting in different local demand patterns.

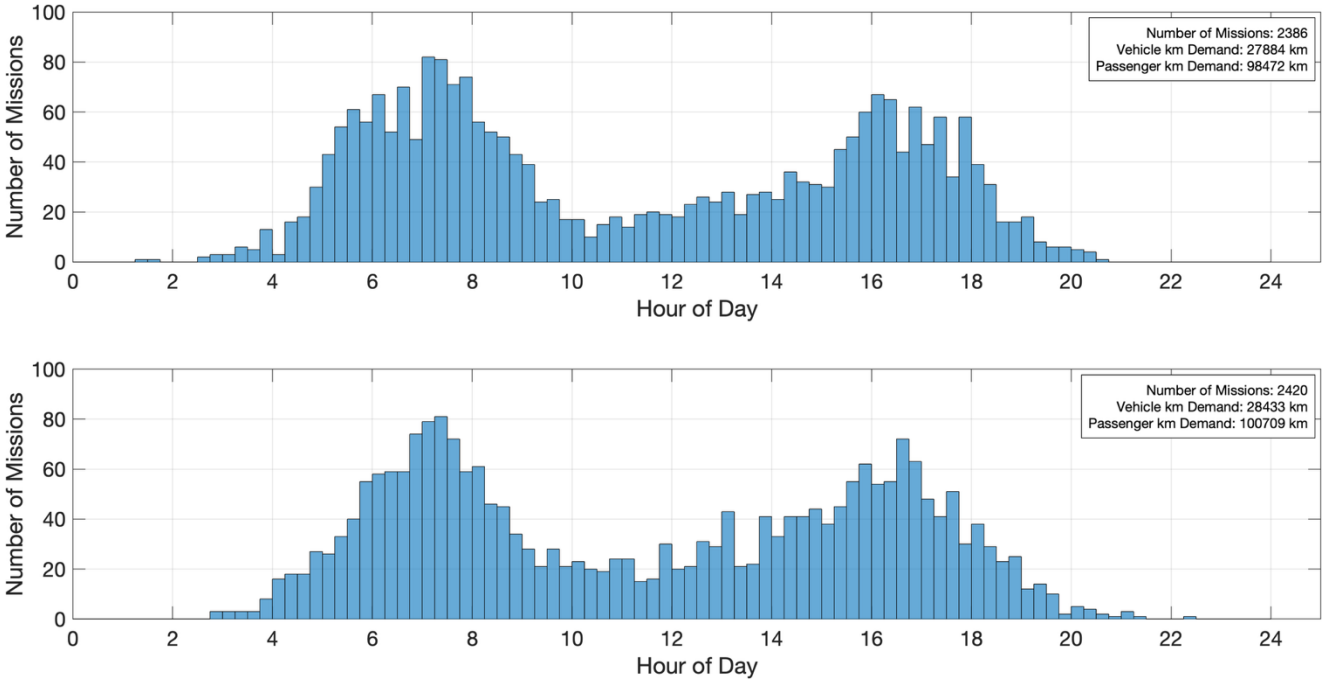


Figure 1 – Temporal distribution of mission demand throughout the day for the investigated scenarios A (top) and B (bottom), derived according to [11,12]. The inset boxes provide the total number of missions together with the corresponding vehicle-kilometer and passenger-kilometer demand used as input for the fleet planning process.

The analyzed fleet consists of tiltrotor vehicle concepts originally introduced in [13]. The same vehicle models and performance assumptions have previously been applied in [9,10], where a detailed description of the vehicle design as well as all relevant performance parameters, including flight speeds, power requirements, and battery capacities, can be found.

2.2 Generation of Vehicle Candidates

The structure of the generated vehicle operating plans, henceforth referred to as mission sequences, is schematically illustrated in Fig. 2. The missions shown in yellow are plotted here as an example excerpt from 8:00 a.m. to 12:00 p.m., based on their departure times. To generate the sequences, the missions are processed in the form of a directed acyclic graph [9]. A single graph is precomputed for each vehicle candidate, taking into account, among other things, flight characteristics such as flight-phase-dependent speeds, as well as the assumed initial position and the earliest time of vehicle

availability. Missions are modeled as pairs of nodes, each representing the start and end of the mission. The edge between the two mission nodes contains information on vehicle-specific energy demand and travel time. Only missions whose passenger demand does not exceed the seat capacity of the vehicle are included. Edges are generated between the end node of one mission and the start node of another mission, provided the temporal constraint is met. Necessary relocation flights, shown in cyan in Fig. 2, are also considered.

Finally, a Longest Path Problem is applied to each graph to generate the sequences by maximizing Revenue Seat Kilometers. In this process, the energy constraint is considered according to

$$E_{Battery\ Charge,Des,n} \geq \Delta E_{Flight:\ DES,n\rightarrow OGN,n+1} + \Delta E_{Flight:\ OGN,n+1\rightarrow DES,n+1} - \left(t_{OGN,n+1} - t_{DES,n} - \Delta t_{Flight:DES,n\rightarrow OGN,n+1}\right) \cdot P_{Charge}. \quad (1)$$

Equation (1) ensures the energetic feasibility of two consecutive missions. The remaining battery energy after mission n, together with the energy that can be recharged before mission n+1, must be sufficient to perform both the required relocation flight and mission n+1. The available charging time is obtained by subtracting the relocation flight time from the time interval between both missions. The energy required to traverse each edge is stored in the graph edges.

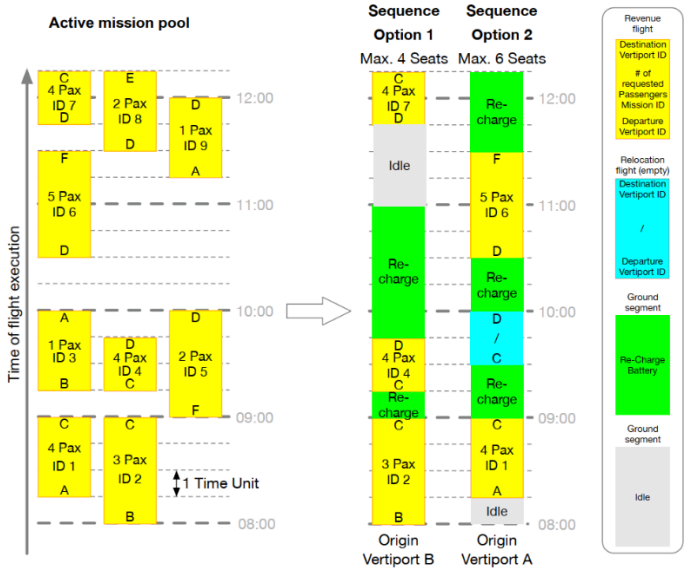


Figure 2 – Schematic representation of vehicle operating plans according to [9]. Sequences consist of productive missions, relocation flights, charging segments, and idle periods, while satisfying temporal, energetic, and vehicle-capacity constraints.

Possible relocation flights between two missions are carried out as late as possible. This approach maintains planning flexibility for potential recalculations of vehicle deployment. At the same time, it must be ensured that, after the relocation flight is completed and before the next mission begins, there is still sufficient time for charging segments (green segments in Fig. 2) to charge the vehicle battery to its maximum achievable state of charge.

2.3 Selection of Vehicle Candidates

After the sequences have been generated, a selection of candidate vehicles is made. In many cases, the sequences of competing candidates contain overlaps from the mission pool. To ensure a unique mission assignment, an assignment problem is formulated as a mixed-integer linear program. The formulation of the constraints also ensures that each vehicle is assigned at most one sequence. In this process, the cost function

$$F_i = C_{Reloc} \cdot T_i^{Reloc} + C_{Idle} \cdot T_i^{Idle} + C_{Char} \cdot T_i^{Char} - w \sum_{j \in M_i} P_j \cdot T_j^{Pax} \quad (2)$$

is minimized.

https://doi.org/10.71945/icas2026_0672

The mission sequences M_i of the candidate vehicles are analyzed with regard to the time spent in each of the four possible sequence phases. These phases include unproductive transfer flights (Reloc), unused downtime on the ground (Idle), battery charging segments (Char), and productive missions with paying passengers. The cost function is composed of the cumulative times T_i^{Phase} of each phase in a sequence and a corresponding weighting factor C_{Phase}. For relocation and idle segments, the factors are set to +1 in each case, so that every unit of time spent in these unproductive states generates a penalty point. Since charging segments are a necessary byproduct of flight operations and can follow both repositioning flights and passenger missions, they do not contribute to the cost function and are assigned the coefficient $C_{Char} = 0$. For each passenger mission j as part of a higher-level sequence M_i, the mission duration T_j^{Pax} is multiplied by the number P_j of passengers transported. This term is incorporated into the cost function as a reward term and is therefore negative. Additionally, this payload term is scaled by a gain factor w to mathematically force productive sequences into the negative range. In the event that the solver finds only the trivial zero solution (all vehicles remain on the ground) due to insufficient weighting, this amplification factor w is iteratively increased until a non-trivial solution is obtained.

2.4 Overall workflow with a rolling-horizon

The submodels described above are integrated into a workflow to quantify the impact of the booking lead time on fleet performance. To do this, the entire day is simulated in a loop using fixed 15-minute time increments. In order to limit computation time and enable parallelization, the mission pool is divided into ten independent subsets containing missions that are approximately evenly distributed throughout the operational day. Each subset is processed separately, and the resulting statistics are aggregated. According to the process shown in Fig. 3, at each time increment, a check is performed to determine whether new entries with $t_{Filing} \leq t_{System}$ have been added to the active pool, which comprises all missions known to the operator.

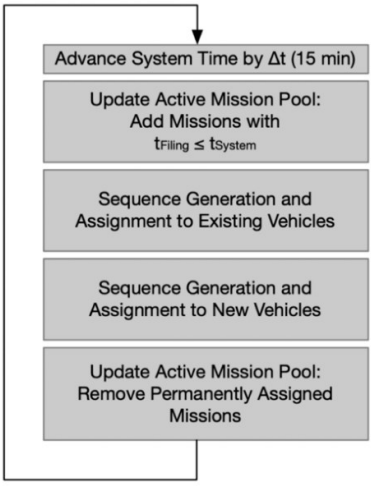


Figure 3. Rolling-horizon fleet planning workflow

First, the missions in the active pool are assigned to existing vehicles in the fleet through sequence generation and solution of the MILP. If the active pool still contains any remaining missions after this assignment, they are assigned to new vehicles.

Before the system time is advanced by a specified time interval (here 15 minutes), all mission sequences are checked to determine which missions must be permanently assigned to their current sequence. A mission is permanently assigned to a sequence as soon as the critical time is reached at which operational preparations must begin. This point in time occurs either when the assigned vehicle must begin a required relocation flight, or—if the vehicle is already at the correct vertiport—30 minutes before the planned mission start time.

3. Results

In this chapter, the impact of booking lead time on fleet size and operational efficiency is first quantified for both scenarios A and B. Subsequently, the impact of vehicle rotations on infrastructure requirements is analyzed with respect to parking positions and charging infrastructure.

3.1 Fleet Analysis

In Fig. 4(a), the resulting fleet size for Scenario A is depicted as a function of booking lead time t_{BL}, ranging from 60 to 180 minutes. The results show that the required fleet size can be significantly reduced as t_{BL} increases. For an increase from 60 to 90 minutes, the resulting fleet size decreases from 358 to 321 vehicles for the same mission volume, corresponding to a reduction of 10%. The minimum fleet size of 297 vehicles is achieved for $t_{BL} = 120$ minutes, corresponding to a reduction of 17%. For longer booking lead times, the required fleet size fluctuates at a similar level between 298 and 301 vehicles.

The results suggest that, for the analyzed network, fleet size reduction potential plateaus once t_{BL} reaches approximately 120 minutes. This value should not be interpreted as a universally applicable threshold, however. It is likely to depend on the average mission duration and the spatial characteristics of the route network. Since mission durations in the scenario under consideration typically range from about 15 to 25 minutes, the observed saturation range corresponds approximately to a booking lead time of four to five times the average mission duration.

In Fig. 4(b), the idle time is depicted over the booking lead time. For $t_{BL} = 60$ minutes, the idle time of the fleet cumulates to 5304 hours throughout the operational day, which equates to an average idle time of 14.8 hours per vehicle. For $t_{BL} = 120$ minutes, the idle time is reduced by 29% to 3765 hours, resulting in 12.7 hours of idle time per vehicle and day. The minimum idle time of 3669 hours (-31%) is achieved at $t_{BL} = 180$ minutes. This reduction exceeds the corresponding fleet size reduction of 17% by 14 percentage points, indicating that the reduction is not exclusively caused by the smaller fleet size, but also by an improvement of temporal vehicle utilization.

The results in Fig. 4(c) show identical revenue seat kilometer (RSK) values for all examined t_{BL} values. This illustrates that the same transport demand is met in all scenarios and that no missions are lost during fleet generation and mission assignment.

The fleet reduction is, however, accompanied by longer transfer distances between consecutive missions, as shown in Fig. 4(d), which depicts the cumulative distance traveled during unproductive relocation flights without passengers. For $t_{BL} = 60$ min, the total relocation distance amounts to 19,590 km. As fleet size decreases with increasing T_{BL}, vehicles in the smaller fleets must relocate more frequently between missions. Consequently, the cumulative relocation distance reaches a maximum of 21,930 km at $t_{BL} = 180$ min, corresponding to an increase of 12%.

The energy demand at the network level is depicted in Fig. 4(e). For $t_{BL} = 60$ minutes, the total energy consumption amounts to approximately 102,000 kWh. As the distance traveled during relocation flights increases with increasing t_{BL}, so does the corresponding energy demand. For $t_{BL} = 180$ min, the energy demand rises to 109,000 kWh, corresponding to an increase of 8%. This increase in energy demand represents a typical consequence of operating a smaller fleet, as additional relocation flights are required between missions

The results for Scenario B, depicted in Fig. 5, are largely consistent with those observed for Scenario A. For $t_{BL} = 60$ min, the resulting fleet comprises 347 vehicles and is therefore slightly smaller than in Scenario A. Nevertheless, the fleet reduction potential and the overall trend with increasing t_{BL} are similar. Increasing t_{BL} to 90 min already reduces fleet size by 13%, while the minimum fleet size of 285 vehicles is achieved for $t_{BL} = 150$ min, corresponding to a reduction of 18%. Similar to Scenario A, the fleet reduction potential is largely exhausted once t_{BL} exceeds 120 min.

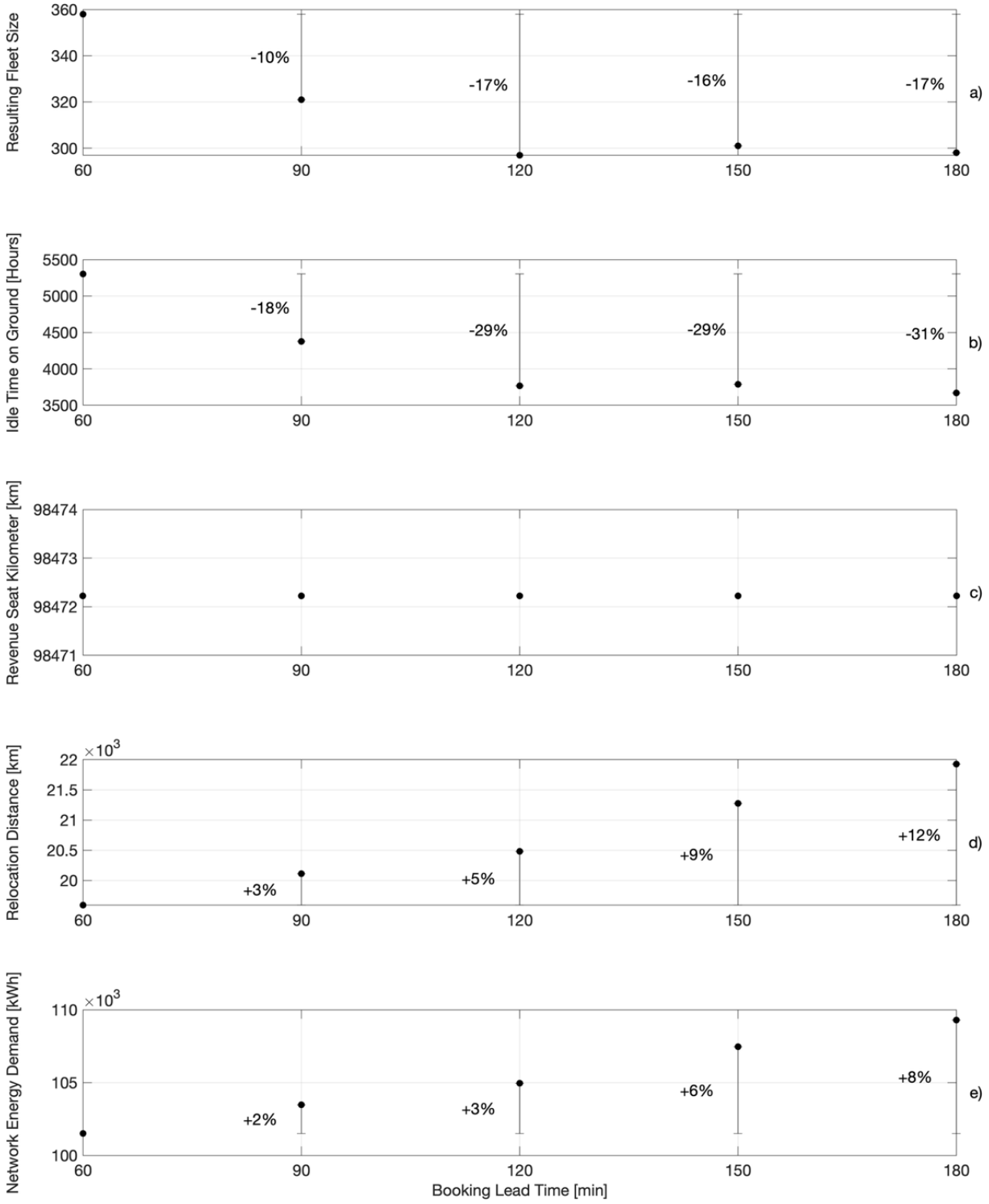


Figure 4. Impact of booking lead time on fleet utilization and operational metrics in Scenario A for t_{BL} values ranging from 60 to 180 min. All relative changes refer to the baseline case of $t_{BL} = 60$ min. Increasing t_{BL} reduces fleet size (-17%) and idle time (-31%), while revenue seat kilometers remain unchanged. These benefits are accompanied by increased relocation distances (+12%) and higher network energy demand (+8%).

The remaining metrics exhibit comparable trends. Idle time is reduced by up to 33%, while relocation distance and energy demand increase by up to 8% and 5%, respectively. Although these relative increases are slightly lower than those observed in Scenario A, both scenarios exhibit comparable absolute values of relocation distance (22,800 km) and energy demand (111,000 kWh) for $t_{BL} =$

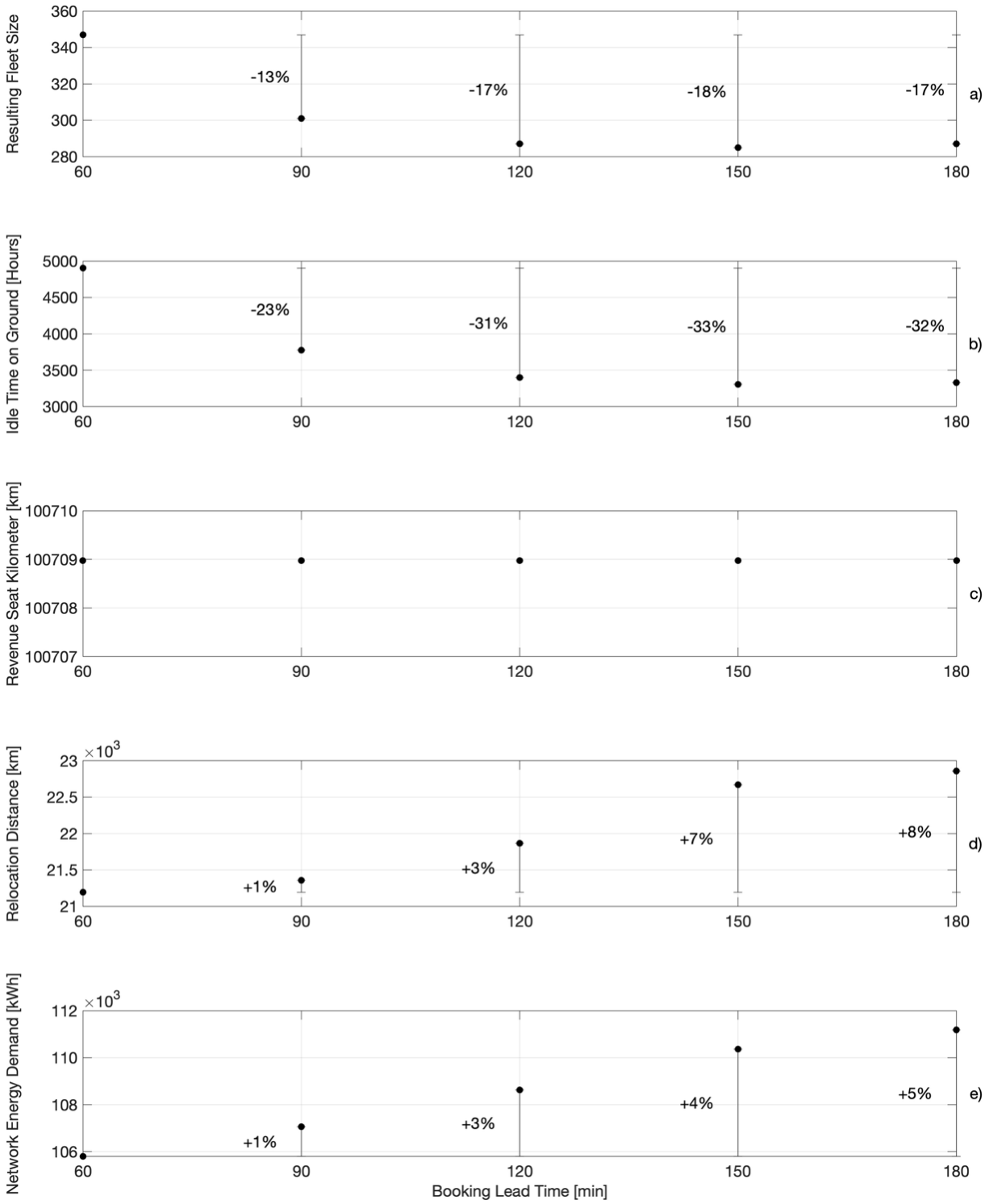


Figure 5. Impact of booking lead time on fleet utilization and operational metrics in Scenario B for t_{BL} values ranging from 60 to 180 min. All relative changes refer to the baseline case of $t_{BL} = 60$ min. Increasing t_{BL} reduces fleet size (-18%) and idle time (-33%), while revenue seat kilometers remain unchanged. These benefits are accompanied by increased relocation distances (+8%) and higher network energy demand (+5%).

180 min. Overall, both analyzed demand scenarios exhibit a comparable fleet reduction potential associated with increased booking lead times. In general, the reduction in fleet size is accompanied by a comparable reduction in fleet seat capacity in both scenarios A and B (see Table 1), indicating that the observed fleet reduction is not primarily achieved by replacing smaller vehicles with larger ones.

Beyond a booking lead time of $t_{BL} = 120$ minutes, however, the sequence generator tends to create

longer operating schedules with additional relocation flights, resulting in increased relocation distances and, consequently, higher energy demand. Furthermore, Table 1 shows that for t_{BL} values beyond 120 minutes, the reduction in fleet seat capacity is slightly smaller than the reduction in the number of vehicles, indicating a tendency towards a higher proportion of larger vehicles in the fleet. Together, these effects contribute to the increased energy demand observed for longer booking lead times.

3.2 Infrastructure Analysis

In this section, the operating schedules of the resulting fleets are analyzed from the perspective of vertiport utilization throughout the operational day. The analysis exclusively focuses on the local demand for parking positions as well as charging power required to implement the respective operating schedules. The resulting peak and average demand therefore provide an indication of the infrastructure capacity required at the vertiports. The scenario with $t_{BL} = 60$ min continues to serve as the reference case. Since the fleet analysis has shown that the largest benefits are already achieved at $t_{BL} = 120$ min, the following analysis focuses on the corresponding operating schedules.

The vertiport network comprises a total of 20 vertiport locations in the Hamburg metropolitan area. In Fig. 6, the infrastructure requirements resulting from the different vehicle operating schedules are first discussed using the example of a selected vertiport located in Rahlstedt.

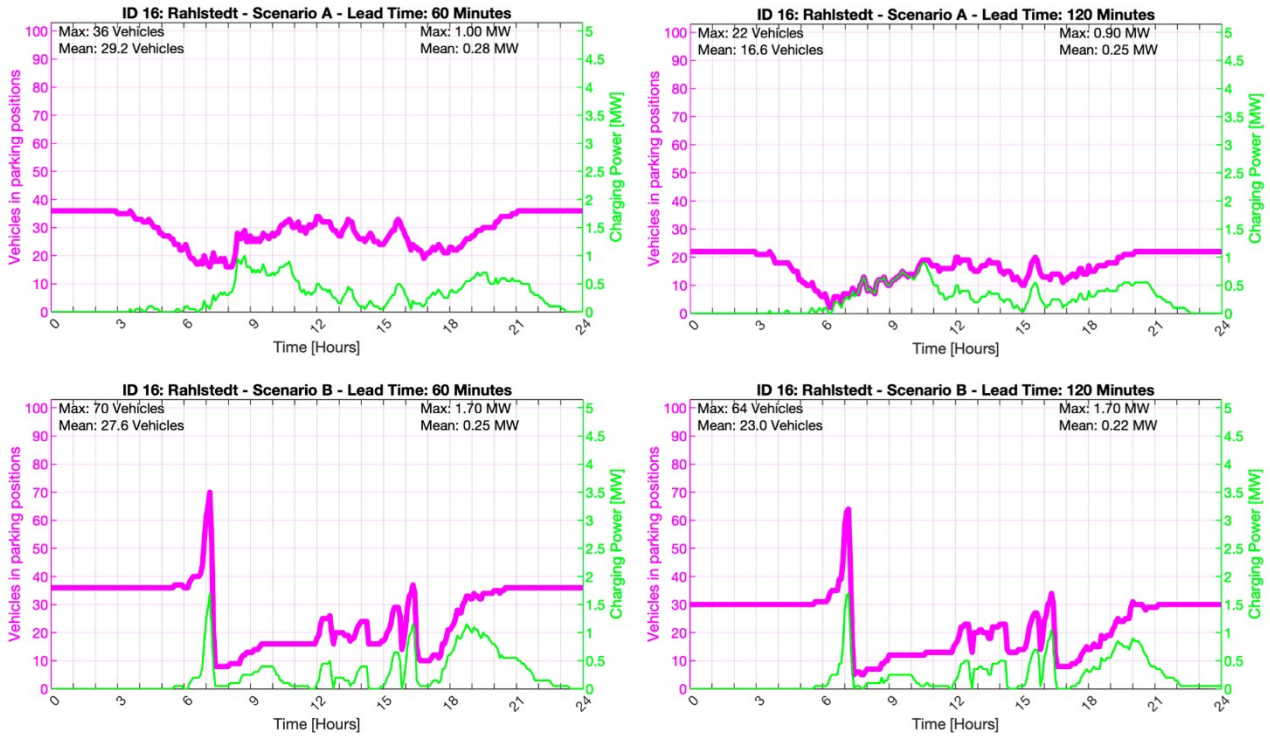


Figure 6. – Daily profile of local parking demand and charging power at the example vertiport in Rahlstedt. The cyan curve indicates the number of vehicles parked at the vertiport, while the green curve shows the local charging power demand. Due to the selected scaling, the number of simultaneously charging vehicles can be directly read from the left-hand axis. Top Left: Scenario A, $t_{BL} = 60$ min. Top Right: Scenario A, t_{BL} =120 min. Bottom Left: Scenario B, t_{BL} =60 min. Bottom Right: Scenario B, t_{BL} =120 min.

Each of the depicted curves shows, in cyan, the number of locally parked vehicles at the vertiport. The top-left plot corresponds to Scenario A with a booking lead time of 60 minutes. At the beginning of the operational day, 36 vehicles are located at the vertiport. With the onset of the morning rush hour at approximately 3:00 a.m., traffic is initially dominated by departing flights. As a result, the

number of parked vehicles decreases to a minimum of 17. During the subsequent hours, arriving traffic dominates until midday, causing the number of parked vehicles to increase again to 35 around noon. Following another minimum in the early evening, the number of vehicles gradually returns to its initial level by the end of the operational day. The cumulative parking demand over the operational day corresponds to an average occupancy of approximately 29 parked vehicles at the Rahlstedt vertiport for Scenario A and $t_{BL} = 60$ min, either charging or remaining idle.

The green curve, referenced to the right-hand axis, shows the charging power of the vehicles located on the ground throughout the operational day.
The scaling of the two curves has been selected such that the charging power can be read from the right-hand axis, while the corresponding number of simultaneously charging vehicles can be determined directly from the left-hand axis. Consequently, the green curve can never exceed the cyan curve. If both curves coincide over a certain period, as observed for Scenario A and $t_{BL} = 120$ min (Fig. 6, top right) between 07:30 a.m. and 10:30 a.m., this indicates that all vehicles present at the vertiport are being charged. A gap between the green and cyan curves, in contrast, corresponds to the number of vehicles remaining in idle mode. For Scenario A and $t_{BL} = 60$ min, the charging power reaches its maximum value of 1 MW at approximately 08:30 a.m., corresponding to 20 simultaneously charging vehicles. The remaining nine vehicles are therefore in idle mode.
A comparison within Scenario A already reveals substantial differences between $t_{BL} = 60$ min and $t_{BL} = 120$ min. It can be observed that, for a booking lead time of 60 minutes, vehicle rotations frequently begin their optimal sequences in Rahlstedt, resulting in a high number of parked vehicles at the vertiport at the beginning of the operational day. Although the number of parked vehicles fluctuates throughout the day, it never falls below 18. Instead, numerous vehicles arrive during the morning hours and are initially charged. However, charging power continuously decreases over the course of the day, while the share of vehicles in idle mode increases.
For $t_{BL} = 120$ min, in contrast, the number of parked vehicles reaches a minimum of only four vehicles at approximately 6:00 a.m. Overall, the comparison of the two rotation plans shows that both the peak and the average parking demand at the Rahlstedt vertiport are significantly reduced for $t_{BL} = 120$ min. The peak demand is reduced to 22 vehicles, while the average parking demand is reduced from 29 to approximately 17 vehicles. In both cases, the average occupancy throughout the day amounts to approximately 81% and 76% of the corresponding peak value, respectively.
Despite the substantial differences in required parking demand, only minor differences in charging power can be observed in this example. For $t_{BL} = 120$ min, the peak charging power is reduced from 1 MW to 0.9 MW. Apart from that, the daily charging profiles are similar in both cases. Based on the local daily average charging power of 0.25 MW, the total energy demand at this vertiport is lower for $t_{BL} = 120$ min than for $t_{BL} = 60$ min, which contrasts with the network-wide trend of a 3% increase in energy demand.

The daily profiles of Scenario B differ substantially from those observed in Scenario A, while showing less distinct differences with respect to t_{BL}. Due to the demand distribution of Scenario B, which assumes a stronger temporal concentration of demand towards individual destinations such as Rahlstedt, pronounced peaks can occur regarding the required parking demand. At approximately 7:00 a.m., parking demand reaches a peak of 70 occupied parking positions for $t_{BL} = 60$ min, while 64 parking positions are still required for $t_{BL} = 120$ min. However, the subsequent outbound traffic causes parking demand to decrease rapidly.

Overall, the two parking demand profiles of Scenario B exhibit very similar characteristics. Due to the short duration of the peak loads, the ratio of average to peak parking demand is only 39% and 36%, respectively, indicating that sizing the parking infrastructure according to peak demand would result in oversized parking capacity for most of the operational day. Only minor differences can also be

observed with respect to charging power. The peak charging power remains unchanged at 1.7 MW for both t_{BL} values.

A comparison of the network-wide charging profiles revealed differences in peak charging power ranging between 11.1 MW (at $t_{BL} = 90$ minutes) and 11.3 MW (at $t_{BL} = 120$ minutes) for Scenario A, and between 10.2 MW (at $t_{BL} = 180$ minutes) and 10.9 MW (at $t_{BL} = 60$ minutes) for Scenario B.

t_{BL}	Scenario A				Scenario B			
	Fleet Vehicle Count	Fleet Seat Count	Peak Parking Demand	Mean Parking Demand	Fleet Vehicle Count	Fleet Seat Count	Peak Parking Demand	Mean Parking Demand
60	**358** (0.0%)	**1506** (0.0%)	**462** (0.0%)	**307** (0.0%)	**347** (0.0%)	**1474** (0.0%)	**911** (0.0%)	**293** (0.0%)
90	**321** (-10.3%)	**1342** (-10.9%)	**443** (-4.1%)	**270** (-12.1%)	**301** (-13.3%)	**1258** (-14.7%)	**890** (-2.3%)	**247** (-15.7%)
120	**297** (-17.0%)	**1256** (-16.6%)	**435** (-5.8%)	**245** (-20.2%)	**287** (-17.3%)	**1220** (-17.2%)	**917** (+0.7%)	**233** (-20.5%)
150	**301** (-15.9%)	**1276** (-15.3%)	**445** (-3.7%)	**249** (-18.9%)	**285** (-17.9%)	**1230** (-16.6%)	**902** (-1.0%)	**231** (-21.2%)
180	**298** (-16.8%)	**1294** (-14.1%)	**441** (-4.6%)	**245** (-20.2%)	**287** (-17.3%)	**1246** (-15.5%)	**911** (-0.0%)	**233** (-20.5%)

Table 1. – Fleet size (number of vehicles and total seat capacity) and cumulative peak parking demand across the vertiport network for different booking lead times t_{BL}

Table 1 summarizes the fleet size and the cumulative local peak parking position requirements across the entire vertiport network. The results clearly show that fleet size decreases significantly with increasing t_{BL} in both Scenarios A and B, whereas the cumulative peak parking position requirements are reduced to a much smaller extent. In Scenario A, a fleet reduction of 17% (358 to 298 vehicles) results in a reduction of 5.8% in the cumulative local peak parking position requirements (462 to 435 positions).

With regard to the mean parking demand, however, $t_{BL} = 120$ minutes provides a reduction potential of 20.2%, which is consistent with the corresponding 29% reduction in idle time, partly compensated by the increase in charging time.

In Scenario B, the peak parking demand remains almost unchanged across all values of t_{BL}, whereas the mean parking demand can be reduced by 20.5% for $t_{BL} = 120$ minutes. The mean parking demand therefore tends to correlate better with the reduction in fleet size. Since optimizing parking and charging infrastructure requirements, both at the local and network level, is not part of the present objective function, the resulting peak demands should be interpreted with caution.

4. Conclusions and Outlook

This study investigated the influence of booking lead time and demand distribution on fleet and infrastructure requirements in an urban air mobility network. For both analyzed demand scenarios, increasing the booking lead time from 60 min to 90 min already results in a substantial fleet reduction of approximately 10-13%, while extending the booking lead time to 120 min increases the fleet reduction potential to approximately 17–18%. Beyond this range, additional benefits become marginal, indicating that most of the achievable operational improvements are already realized at booking lead times between 90 and 120 min.

The results further demonstrate that the reduction in fleet size is primarily enabled by improved temporal vehicle utilization. While the operating plans derived for higher booking lead times often require additional relocation activity, the associated increase in network-wide energy demand

remains comparatively small. Consequently, the operational benefits resulting from improved planning flexibility appear to outweigh the additional relocation effort. From an operator perspective, booking lead times between 90 and 120 min may represent an attractive compromise between operational efficiency and passenger flexibility. Ultimately, the preferred booking lead time should be evaluated from a monetary perspective. However, considering the potential reductions in fleet acquisition, maintenance, parking, and charging infrastructure requirements, the observed fleet reductions appear promising while maintaining identical transport demand.

In the present study, the sequence generation focuses exclusively on fleet optimization. Consequently, no dedicated measures are implemented to reduce local parking or charging peaks, such as operational holding strategies, relocation concepts, or coordinated arrival management. The comparison of Scenarios A and B demonstrates that similar fleet sizes can be associated with substantially different local parking requirements. Consequently, infrastructure sizing based on a single demand scenario should be interpreted with caution. The peak parking requirements presented in this study should therefore not be interpreted as minimum infrastructure requirements, but rather as the peak demand resulting from the current fleet optimization approach. In contrast, the mean local parking demand shows a considerably stronger dependency on booking lead time and may therefore provide a more suitable basic indicator for estimating local infrastructure requirements.

Future work should further investigate the mechanisms that drive fleet size and infrastructure requirements in UAM networks. In particular, the influence of different demand distributions, network topologies, and operational concepts should be analyzed in greater detail. Furthermore, integrated optimization approaches that jointly consider fleet operations and vertiport infrastructure should be developed. In particular, operational concepts for mitigating peaks in parking and charging demand should be investigated. Another promising direction is the investigation of mixed booking lead time concepts, allowing passengers to choose between higher planning flexibility at increased cost or longer booking lead times with lower operational cost. Finally, the observed saturation of fleet reduction beyond booking lead times of approximately 120 minutes should be validated for different network topologies and mission characteristics. In particular, it should be investigated whether the observed plateau is generally related to the average mission duration or represents a characteristic of the investigated network and optimization approach. Furthermore, future work should investigate the achievable benefits of intraday demand forecasting, for instance by incorporating weather conditions, seasonal effects, and historical operator data. Such forecasting capabilities may complement or partially replace the planning flexibility gained through longer booking lead times by improving knowledge of upcoming transport demand.

Contact Author Email Address

Contact author: Majed.Swaid@dlr.de

Copyright Statement

The authors confirm that they, and/or their company or organization, hold copyright on all of the original material included in this paper. The authors also confirm that they have obtained permission, from the copyright holder of any third party material included in this paper, to publish it as part of their paper. The authors confirm that they give permission, or have obtained permission from the copyright holder of this paper, for the publication and distribution of this paper as part of the ICAS proceedings or as individual off-prints from the proceedings.

References

[1] Maget, C., Gutmann, S. and Bogenberger, K., “Model-based Evaluations Combining Autonomous Cars and a Large-scale Passenger Drone Service: The Bavarian Case Study,“ 2020 IEEE 23rd International Conference on Intelligent Transportation Systems, ITSC 2020. 2020.

[2] Wu, Z. and Zhang, Y., “Integrated Network Design and Demand Forecast for On-Demand Urban Air Mobility,“ Engineering. 2021.

[3] Venkatesh, N., Payan, A. P., Justin, C. Y., Kee, E. and Mavris, D. N., “Optimal siting of sub-urban air mobility (Suam) ground architectures using network flow formulation,“ AIAA AVIATION 2020 FORUM. 2020.

[4] Zelinski, S., “Operational analysis of vertiport surface topology,“ AIAA/IEEE Digital Avionics Systems Conference – Proceedings. 2020.

[5] Vascik, P. D. and Hansman, R. J., “Development of vertiport capacity envelopes and analysis of their sensitivity to topological and operational factors,“ AIAA Scitech 2019 Forum. 2019.

[6] Kleinbekman, I. C., Mitici, M. A. and Wei, P., “eVTOL arrival sequencing and scheduling for on-demand urban air mobility,“ AIAA/IEEE Digital Avionics Systems Conference – Proceedings. 2018.

[7] Zare, Z., Karatas, M. and Zheng, Y.-J., “A Capacitated Set Cover Formulation for Vertiport Location and Air Taxi Allocation,“ Proceedings of the 10th North Americal International Conference on Industrial Engineering and Operations Management, Orlando, Florida, USA, June 17-19, 2025.

[8] Macias, J. E., Khalife, C., Slim, J. and Angeloudis, P., “An integrated vertiport placement model considering vehicle sizing and queuing: A case study in London,“ Journal of Air Transport Management – Volume 113, September 2023, 102486.

[9] Swaid, M., Pertz, J., Niklaß, M., and Linke, F., “Optimized capacity allocation in a UAM vertiport network utilizing efficient ride matching,“ AIAA Aviation 2023 Forum, San Diego, California. 2023.

[10] Swaid, M., Papakonstantinou, S., Kloock-Schreiber, D., Linke, F. and Gollnick, V., “Design of a UAM Ground Infrastructure Network with Respect to Maintenance Capacity Requirements,“ 34th Congress of the International Council of the Aeronautical Sciences, ICAS 2024, September 9-13, Florence, Italy, 2024.

[11] Pertz, J., Lütjens, K. and Gollnick, V., “Approach of modeling passenger’s commuting behavior for UAM traffic in Hamburg, Germany,” In 25th ATRS World Conference. Symposium conducted at the meeting of ATRS, Antwerpen, Belgium.

[12] Pertz, J., Lütjens, K., and Gollnick, V., “Evaluation of business travel as a potential customer field of a local AAM market”, In 26th ATRS World Conference. Symposium conducted at the meeting of ATRS, Kobe, Japan.

[13] Ratei, P., Naeem, N., and Prakasha, P.S., “Development of an Urban Air Mobility Vehicle Family Concept by System of Systems Aircraft Design and Assessment,” 12th EASN International Conference, 18-21. Oct 2022, Barcelona, Spain.